Multidimensional pump-probe spectroscopy with entangled twin-photon states

Oleksiy Roslyak* and Shaul Mukamel†
Department of Chemistry, University of California, Irvine, California 92697-2025, USA
(Received 18 February 2009; published 17 June 2009)

We show that entangled photons may be used in coherent multidimensional nonlinear spectroscopy to provide information on matter by scanning photon wave function parameters (entanglement time and delay of twin photons), rather than frequencies and time delays, as is commonly done with classical pulses. Signals are expressed and interpreted intuitively in terms of products of matter and field correlation functions using a diagrammatic close time path loop formalism which reveals the entangled quantum pathways of the fields and matter. The pump-probe signal measured when the pump and the probe are in a twin entangled state shows two-photon resonant contributions which scale linearly rather than quadratically with the incident beam intensity and reveal frequencies of off-resonant transitions. Two-dimensional spectrograms obtained by double Fourier transform of the signal with respect to the entanglement time and delay of the twins could provide detailed information on correlations among states and dynamical processes with high temporal resolution. The analogy with multidimensional time-domain optical techniques which use sequences of short classical pulses and pulse shaping algorithms is pointed out.

DOI: 10.1103/PhysRevA.79.063409 PACS number(s): 32.80.Qk, 33.80.Wz

I. INTRODUCTION

Multidimensional techniques have long been used in NMR to study the structure and dynamics of complex molecules by measuring the response of spins to sequences of magnetic pulses [1]. Correlation plots obtained by varying several time delays spread the information in multiple dimensions thus improving the resolution and obtaining information unavailable from ordinary one-dimensional (1D) spectroscopy (e.g., absorption). Over the past 15 years these techniques have been extended to the femtosecond regime using infrared and visible pulses [2–4] and were applied to many types of systems and relaxation processes including vibrations in proteins, protein folding, hydrogen bonded liquids, and exciton dynamics in electronically excited photosynthetic complexes [5]. Pulse shaping techniques make it possible to manipulate and control these signals [6–11]. All of these measurements employ classical fields and use multiple pulse delays or frequencies as control parameters.

In this paper we propose multidimensional signals which exploit the quantum nature of the field and are based on the manipulation of photon wave functions. These can now be engineered to create entangled photons which depend on multiple parameters that can be varied to generate two-dimensional (2D) correlation spectra. Entanglement is a purely quantum type of correlation among particles which exists even when they are spatially well separated [12,13]. Many applications to quantum computing, information and communication protocols, cryptography, and teleportation are based on the manipulation of entangled particles [14–16]. Nonlocal quantum correlations brought about by entanglement have been used to test the foundations of quantum mechanics by demonstrating violation of Bell's inequalities and resolving the Einstein-Podolsky-Rosen (EPR) paradox [17–19]. It is easier to maintain entanglement of photons than of massive particles. Entangled photons have been generated by a variety of schemes. These include atomic cascades [20–22], parametric down conversion (PDC) [23,24], or hyperparametric scattering (HPS) [25,26] in nonlinear crystals and, most recently, biexciton decay in semiconductors [27,28]. The photons may be entangled with respect to their polarization, momentum-position, energy-time, their orbital angular momentum, or number state. Photons may be hyperentangled when the entanglement is encoded in several degrees of freedom all mentioned above [29,30].

Entangled photons have been used recently in nonlinear spectroscopic applications, including two-photon absorption (TPA) [31,32,53], sum frequency generation (SFG) [33–35], two-photon-induced fluorescence (TPIF) [36–40], and two-photon-induced transparency (TPIT) [41]. The simplest signature of entanglement is that TPA signals scale linearly rather than quadratically with the pump intensity [42]. This reflects the fact that in these experiments, the entangled photons act as a single object. This effect has been predicted and demonstrated in molecular systems. As a consequence, power levels required for TPA excitation can be dramatically reduced by many orders of magnitude, becoming closer to those for single-photon excitation [36]. This could be used to minimize damage in two-photon microscopy. The spatial resolution can also be improved since TPA only takes place in regions where correlated photon pairs overlap in space and time [43,44].

In a recent study we calculated pump-probe (PP) signals using polarization entangled photons generated by type II PDC and postselected by the Mach-Zehnder interferometer. We showed that only the TPA pathways scale linearly with pump intensity and at low pump intensity dominate the other, stimulated Raman (SR) contributions, which scale quadratically. Thus the entangled photons enable quantum pathway selectivity and can help disentangle complex spectra with overlapping features [45]. Photon-entanglement-induced strong correlations of quantum pathways of matter have also

*oroslyak@uci.edu
†smukamel@uci.edu

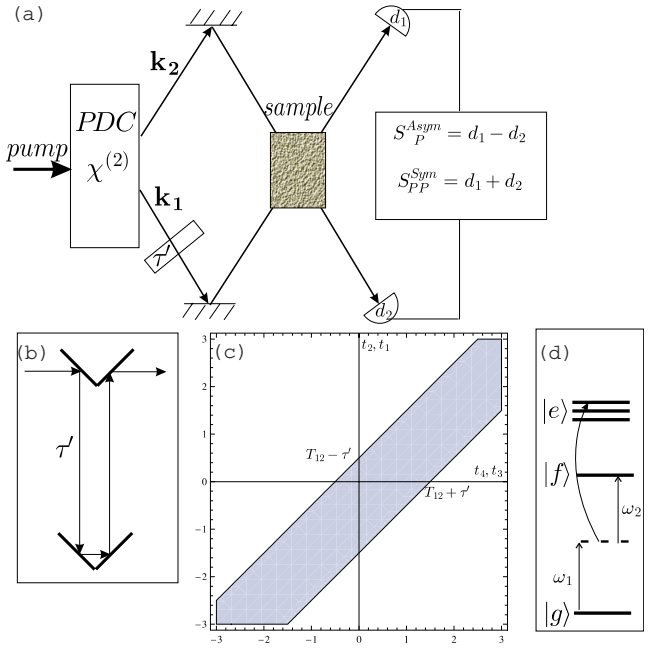

FIG. 1. (Color online) (a) Pump-probe experiment with the twin photons. (b) One of the possible schemes for controlling the external time delay τ between the twins [40]. (c) The twin photon transition amplitude in Eq. (22) is nonzero in the diagonal strip of width $\sqrt{2}T_{12}$. The symmetry of photon interactions $t_4 \leftrightarrow t_2, t_3 \leftrightarrow t_1$ is broken when one of them is delayed. (d) The model molecular level scheme used in our simulations.

been predicted for the difference frequency generation (DFG) technique [46].

Here we focus on a different type of entangled two-photon states known as "twin photons" [40,41,47,54]. The twins are generated by PDC of a single pump photon and correlated both in time and space. Their TPA which occurs within the entanglement time T_{12} and area A_{12} is strongly enhanced since it does not rely on the accidental simultaneous arrival of two uncorrelated photons. TPA with twin photons had also been used to detect off-resonant states. The sample becomes transparent for certain values of the entanglement time T_{12}, thereby revealing off-resonant state frequencies. Alternatively, one can fix the entanglement time and introduce a time delay $|\tau| \leq T_{12}$ between the twin photons. The Fourier transform of the TPA signal with respect to τ can also reveal the structure of the virtual states. Since the delay can be varied with 0.25 fs steps, the technique can monitor intermediate-state levels separated by ~eV and may therefore be used for atomic spectroscopy. Current theory is limited to the regime where the entangled time is shorter than the dephasing time [32]. We develop a microscopic theory of nonlinear optical signals with twin photons using close time path loop (CTPL) diagrams [48,49] and apply it to predict pump-probe signals in a three-level ladder $|g\rangle, |e\rangle, |f\rangle$ (Fig. 1). We focus on resonances in PP spectroscopy where the sum of the pump and probe frequencies is resonant with one of the molecular states $|f\rangle$ i.e., $\omega_1 + \omega_2 = \omega_{fg}$. Difference frequency $\omega_1 - \omega_2$ (stimulated Raman) type resonances are interesting as well, but will not be considered here. In Sec. II we show that the signals for general quantum optical fields are given by sums over products of matter and light quantum pathways. The pathways can be divided into two groups. The first, representing TPA, is expressed as a modulus square of a two-photon scattering amplitude (T matrix) $\sim |\mathcal{T}_{fg}(T_{12}, \tau)|^2$. It may be calculated as two-photon counting rate using Glauber's theory [23,39,50]. The second component [pump modulated probe (PMP)] represents a process where the pump acts as a "catalyst." It modulates the probe absorption but returns to its initial state at the end. This group is given by the imaginary part of an amplitude product $\sim \mathcal{T}^{\star}_{gf}\mathcal{T}^{\star}_{fg}$ (not modulus square) and cannot be calculated as a photon counting rate. The TPA and PMP can be measured separately by fluorescence from the doubly excited $|f\rangle$ and the singly excited states $|e\rangle$, respectively. Each group has a characteristic resonances pattern. In Sec. III we show that the TPA and PMP contributions to the signal are identical when the fields are classical and the intermediate state $|e\rangle$ is off resonant. In Sec. IV we study the variation of the signal with the entanglement time T_{12}. We show that the TPA signal with twin photons scales linearly with the field intensity and is inversely proportional to the entanglement time. In Sec. V we introduce the time delay τ between the twins and present 2D correlation spectra obtained by a double Fourier transform with respect to the entanglement time T_{12} and τ. Various groups of resonances can be clearly separated by these spectra which contain a rich pattern of cross peaks. In Sec. VI we discuss the connection with 2D signals obtained with shaped classical pulses. We show that two mutually delayed rectangularly

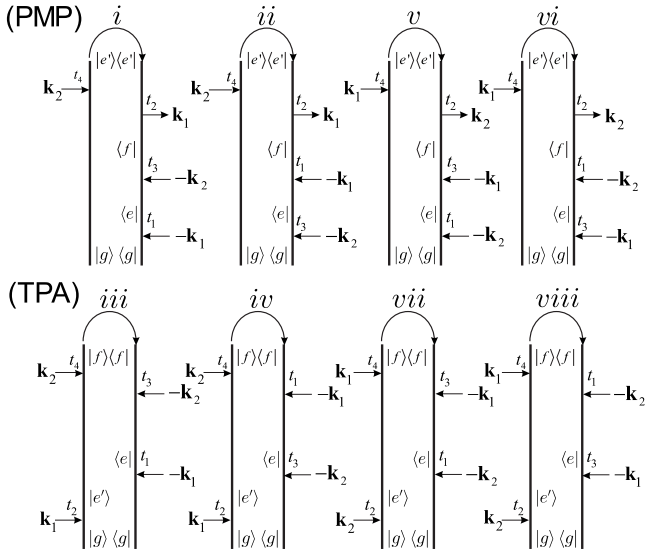

FIG. 2. CTPL diagrams for the contributions to the pump-probe signal which contain $\omega_1 + \omega_2 = \omega_{fg}$ resonances. By convention, the last interaction is an absorption and occurs at the left branch of the loop. Diagrams i–iv represent $\mathbf{k}_1$ (pump) and $\mathbf{k}_2$ (probe) [v–vii are $\mathbf{k}_1$ (probe) and $\mathbf{k}_2$ (pump)]. The top row diagrams represent pump modulated probe (PMP) where the system ends in the singly excited state $|e\rangle\langle e|$. The bottom row diagrams represent two-photon absorption (TPA) where the matter ends in the doubly excited state $|f\rangle\langle f|$.

shaped optical fields may be used to reproduce the TPA spectra obtained with twins. A general discussion is finally given in Sec. VII.

II. CTPL FORMALISM OF PUMP-PROBE SIGNALS

We consider an assembly of N three-level $|g\rangle,|e\rangle,|f\rangle$ molecules [Fig. 1(d)] which are initially in the ground state $|g\rangle$. We focus on one component of a general PP signal obtained with two optical modes $\mathbf{k}_1$ and $\mathbf{k}_2$ where the sum of the two-photon frequencies coincides with one of the transitions $\omega_1+\omega_2=\omega_{gf}$. The stimulated Raman part with $\omega_1-\omega_2$ resonances is neglected. The frequency domain (cw) PP signal with classical modes is defined as the change in the transmitted intensity of the probe with and without the pump [48]. We treat both beams on the same footing as shown in Fig. 1(a). One of the detectors (d_2) measures the change in intensity of the "probe" mode E_2 with and without the sample. The second detector (d_1) does the same for the "pump" mode E_1. We thus define two signals:

$$S_{\mathrm{PP}}^{d_2}(\omega_2;\omega_1) = -\,\mathrm{Im}\frac{N}{T}\int_{-T}^{T} dt_4\langle E_2^{\dagger}(t_4)P^{(3)}(\mathbf{k}_2,t_4)\rangle, \qquad (1)$$

$$S_{\mathrm{PP}}^{d_1}(\omega_1;\omega_2) = -\,\mathrm{Im}\frac{N}{T}\int_{-T}^{T} dt_4\langle E_1^{\dagger}(t_4)P^{(3)}(\mathbf{k}_1,t_4)\rangle. \qquad (2)$$

Here $P^{(3)}(\mathbf{k},t)$ is the third-order polarization and $2T$ is the measurement time. The nonlinear polarization is induced by sequence of interactions with the optical fields. When the last interaction occurs with $\mathbf{k}_2$ ($\mathbf{k}_1$) mode it gives $P^{(3)}(\mathbf{k}_2,t_4)$ $[P^{(3)}(\mathbf{k}_1,t_4)]$.

We further define the following symmetric and asymmetric combinations of the two signals:

$$S_{\mathrm{PP}}^{\mathrm{Sym}}(\omega_1;\omega_2) = \tfrac{1}{2}[S_{\mathrm{PP}}^{d_1}(\omega_1;\omega_2) + S_{\mathrm{PP}}^{d_2}(\omega_2;\omega_1)],$$

$$S_{\mathrm{PP}}^{\mathrm{Asym}}(\omega_1;\omega_2) = \tfrac{1}{2}[S_{\mathrm{PP}}^{d_1}(\omega_2;\omega_1) - S_{\mathrm{PP}}^{d_2}(\omega_1;\omega_2)]. \qquad (3)$$

In the rotating wave approximation the matter field coupling is given by

$$H_{\mathrm{int}} = V^{\dagger}(t)E(t) + V(t)E^{\dagger}(t).$$

Here the dipole operator is partitioned as $V(t)+V^{\dagger}(t)$, where

$$V(t) = \sum_j \sum_{k>j} \mu_{jk} e^{i\omega_{jg}t}|j\rangle\langle k|e^{-i\omega_{kg}t} \qquad (4)$$

is the positive frequency (de-excitation) part; $\{|k\rangle\}$ represents the eigenstates of the bare material system labeled according to increasing energy. $V^{\dagger}$ represents the excitation part of the dipole operator.

The field of mode $j=1,2$ is similarly partitioned as $E_j(t)+E_j^{\dagger}(t)$, where the positive frequency component is

$$E_j(t) = \left(\frac{2\pi\omega_j}{\Omega}\right)^{1/2} a_j \exp(-i\omega_j t). \qquad (5)$$

Here, a_j ($a_j^{\dagger}$) is the annihilation (creation) boson operator for the j mode and Ω is the quantization volume.

Using the superoperator nonequilibrium Green's function (SNGF) formalism [48,51] and the loop diagrams of Fig. 2 we can express Eq. (1) in terms of four-point correlation function of the matter and the field and obtain

$$\begin{aligned} S_{\mathrm{PP}}^{d_2}(\omega_2;\omega_1) = -\frac{2N}{T}\int_{-T}^{T} dt_4\ \mathrm{Im}\ i^3\int_{-\infty}^{\infty}\int_{-\infty}^{\infty}\int_{-\infty}^{\infty} dt_3 dt_2 dt_1[\,&\theta(t_4-t_2)\theta(t_2-t_3)\theta(t_3-t_1)\langle V(t_1)V(t_3)V^{\dagger}(t_2)V^{\dagger}(t_4)\rangle \\ &\times\langle E_1^{\dagger}(t_1)E_2^{\dagger}(t_3)E_1(t_2)E_2(t_4)\rangle + \theta(t_4-t_2)\theta(t_2-t_1)\theta(t_1-t_3)\langle V(t_3)V(t_1)V^{\dagger}(t_2)V^{\dagger}(t_4)\rangle\langle E_2^{\dagger}(t_3)E_1^{\dagger}(t_1)E_1(t_2)E_2(t_4)\rangle \\ &+ \theta(t_4-t_2)\theta(t_4-t_3)\theta(t_3-t_1)\langle V(t_1)V(t_3)V^{\dagger}(t_4)V^{\dagger}(t_2)\rangle\langle E_1^{\dagger}(t_1)E_2^{\dagger}(t_3)E_2(t_4)E_1(t_2)\rangle \\ &+ \theta(t_4-t_2)\theta(t_4-t_1)\theta(t_1-t_3)\langle V(t_3)V(t_1)V^{\dagger}(t_4)V^{\dagger}(t_2)\rangle\langle E_2^{\dagger}(t_3)E_1^{\dagger}(t_1)E_2(t_4)E_1(t_2)\rangle]. \end{aligned} \qquad (6)$$

Here the step functions $\theta(t-\tau)$ maintain the time orderings of interactions along the loop (but not in real time). The interactions are time ordered within each branch of the diagram, but the two branches are not time ordered with respect to each other. By convention, the chronologically last interaction is an absorption and occurs at the left branch of the loop. The four terms in Eq. (6) correspond to diagrams i–iv of Fig. 2. $S_{\mathrm{PP}}^{d_1}(\omega_1;\omega_2)$ is given by diagrams v–vii and can be obtained from $S_{\mathrm{PP}}^{d_2}(\omega_2;\omega_1)$ [Eq. (6)] by interchanging $\{\omega_1\leftrightarrow\omega_2\}$. To proceed further we must calculate the optical field correlation functions by specifying its initial state.

III. PUMP-PROBE SPECTROSCOPY WITH CLASSICAL OPTICAL FIELDS

To set the stage and introduce the relevant building blocks of the signal we shall first consider conventional frequency domain PP performed with classical modes. In this case all optical field correlation functions in Eq. (6) may be factorized into the same product of the field intensities: $\langle E^{\dagger}E^{\dagger}EE\rangle=|\mathcal{E}_1|^2|\mathcal{E}_2|^2$. The time arguments in the optical field correlation functions transformed to the loop times (the arguments of the step functions) provide the Fourier compo-

nents of the material correlation functions and yield the signal

$$S^{d_1}_{\mathrm{PP}}(\omega_1;\omega_2) = 4N|\mathcal{E}_1|^2|\mathcal{E}_2|^2 \ \mathrm{Im}\ \chi^{(3)}(-\omega_1;\omega_1,-\omega_2,\omega_2),$$

$$S^{d_2}_{\mathrm{PP}}(\omega_2;\omega_1) = 4N|\mathcal{E}_1|^2|\mathcal{E}_2|^2 \ \mathrm{Im}\ \chi^{(3)}(-\omega_2;\omega_2,-\omega_1,\omega_1),$$

where the explicit CTPL expression for nonlinear susceptibility $\chi^{(3)}$ is given in Refs. [48,49]. For comparison with the entangled photon generated PP signal we recast the above expressions in terms of elements of the symmetric two-photon scattering T matrix,

$$\mathcal{T}(\omega_1,\omega_2) = (V+V^\dagger)[G(\omega_1+\omega_g)+G(\omega_2+\omega_g)](V+V^\dagger), \tag{7}$$

where $G(\omega)$ is the Fourier transform of the retarded Green's function operator $G(\tau)=\theta(\tau)\exp(-iH\tau)$,

$$G(\omega) = -i\int_{-\infty}^{\infty} d\tau\, G(\tau)e^{i\omega\tau},$$

where H is the matter Hamiltonian. We shall need the following matrix elements of the two-photon operator (two-photon transition amplitudes):

$$\langle f|\mathcal{T}(\omega_1,\omega_2)|g\rangle = \mathcal{T}_{fg}(\omega_1,\omega_2) = \mu^\star_{fe}I_{eg}(\omega_1)\mu^\star_{eg} + \mu^\star_{fe}I_{eg}(\omega_2)\mu^\star_{eg},$$

$$\begin{aligned}\langle f|\mathcal{T}^\dagger(\omega_1,\omega_2)|g\rangle &= \mathcal{T}^\star_{fg}(\omega_1,\omega_2)\\ &= \mu^\star_{fe}I^\star_{eg}(\omega_1)\mu^\star_{eg} + \mu^\star_{fe}I^\star_{eg}(\omega_2)\mu^\star_{eg},\end{aligned}$$

$$\langle g|\mathcal{T}(\omega_1,\omega_2)|f\rangle = \mathcal{T}_{gf}(\omega_1,\omega_2) = \mu_{ge}I_{ge}(\omega_1)\mu_{ef} + \mu_{ge}I_{ge}(\omega_2)\mu_{ef},$$

$$\begin{aligned}\langle g|\mathcal{T}^\dagger(\omega_1,\omega_2)|f\rangle &= \mathcal{T}^\star_{gf}(\omega_1,\omega_2)\\ &= \mu_{ge}I^\star_{ge}(\omega_1)\mu_{ef} + \mu_{ge}I^\star_{ge}(\omega_2)\mu_{ef}.\end{aligned} \tag{8}$$

Here we have introduced the auxiliary quantity

$$I_{eg}(\omega) = G_{ee}(\omega+\omega_g) = \frac{1}{\omega-\omega_{eg}+i\gamma}, \tag{9}$$

where $G_{ee}(\tau)=\theta(\tau)\exp(-i\omega_e\tau-\gamma\tau)$, γ is a dephasing rate, and $\exp(i\omega_g\tau)$ describes the free evolution of the molecule in the ground state $|g\rangle$.

$\mathcal{T}_{fg}(\omega_1,\omega_2)$ describes retarded TPA on the left branches of the loop diagrams in Fig. 2 where the loop time runs forward. $\mathcal{T}^\star_{fg}(\omega_1,\omega_2)$ represents advanced TPA on the right branches where the loop time runs backward. Similarly, $\mathcal{T}_{gf}(\omega_1,\omega_2)$ $[\mathcal{T}^\star_{gf}(\omega_1,\omega_2)]$ describes retarded (advanced) TP emission. The system evolution after the absorption of the two photons is described by the doubly excited state Green's function $G_{ff}=\theta(\tau)\exp(-i\omega_f\tau)$ and we define

$$I_{fg}(\omega_1+\omega_2) = G_{ff}(\omega_1+\omega_2+\omega_g) = \frac{1}{\omega_1+\omega_2-\omega_{fg}+i\gamma}. \tag{10}$$

Using the loop diagram rules [48] and Eq. (9) we obtain

$$\begin{aligned}S^{d_2}_{\mathrm{PP}}(\omega_2;\omega_1) \sim \mathrm{Im}\ i^6\sum_{e'e}\mu_{ge'}\mu^\star_e\mu_{e'f}\mu^\star_{fe}I^\star_{fg}(\omega_1+\omega_2)\\ \times[I^\star_{e'g}(\omega_2)I^\star_{eg}(\omega_1)+I^\star_{e'g}(\omega_2)I^\star_{eg}(\omega_2)\\ +I_{e'g}(\omega_1)I^\star_{eg}(\omega_1)+I_{e'g}(\omega_1)I^\star_{eg}(\omega_2)].\end{aligned}$$

The four terms correspond to pathways i–iv in Fig. 2, respectively. The other signal $S^{d_1}_{\mathrm{PP}}(\omega_1;\omega_2)$ can be obtained from the above equation by interchanging ω_1 and ω_2.

The symmetric signal (3) assumes a compact form in terms of the two-photon transition amplitudes (8),

$$\begin{aligned}S^{\mathrm{Sym}}_{\mathrm{PP}}(\omega_1,\omega_2) &= S_{\mathrm{PMP}}(\omega_1;\omega_2)+S_{\mathrm{TPA}}(\omega_1;\omega_2)\\ &\equiv 2N|\mathcal{E}_1|^2|\mathcal{E}_2|^2\mathrm{Im}\ I^\star_{fg}(\omega_1+\omega_2)\\ &\times[\mathcal{T}^\star_{gf}(\omega_1,\omega_2)\mathcal{T}^\star_{fg}(\omega_1,\omega_2)+|\mathcal{T}_{fg}(\omega_1,\omega_2)|^2].\end{aligned} \tag{11}$$

The two terms in the brackets represent the PMP and TPA groups of pathways, respectively, as shown in Fig. 2. To interpret these terms we recall that PP is accompanied by spontaneous light-emission process. Each partially time-ordered CTPL diagram may be dissected into a set of fully time-ordered Feynman diagrams, where chronologically the last interaction occurs at time t_4 [52]. In the TPA pathways the molecule ends up in the doubly excited state $|f\rangle\langle f|$ and two photons are absorbed. The fluorescence from this state can be detected and described by the TP counting [50] formalism $\sim|\mathcal{T}_{fg}|^2$. The fundamental difference between the single-photon absorption and the PMP is the involvement of the second photon. The state of the second mode at time t_4 is the same as its initial state, but it provides intermediate coherence between the ground and double excited states, i.e., catalyzes the absorption of the other mode. The PMP pathways are related to fluorescence from the intermediate states $|e\rangle\langle e|$. Since only one of the photons is absorbed, their contribution is not described by the single-photon transition amplitude as in the photon counting formalism but by $\sim\mathcal{T}^\star_{gf}(\omega_1,\omega_2)\mathcal{T}^\star_{fg}(\omega_1,\omega_2)$.

The asymmetric signal vanishes in the degenerate case $(\omega_1=\omega_2)$ where the two detectors give the same PP signal. When the intermediate states $|e\rangle$ are off resonant one has $T^\star_{fg}(\omega_1,\omega_2)=T_{fg}(\omega_1,\omega_2)$. Equation (11) then assumes the two-photon counting form

$$S^{\mathrm{Sym}}_{\mathrm{PP}}(\omega_1,\omega_2) = 4N|\mathcal{E}_1|^2|\mathcal{E}_2|^2|\mathcal{T}_{gf}(\omega_1,\omega_2)|^2\delta(\omega_1+\omega_2-\omega_{fg}).$$

However, as will be shown in Sec. IV, these results do not hold for quantum optical fields, where the two photons are correlated. Additional terms coming from the PMP group of pathways contribute to all PP signals. As a result, spontaneous emission from the final $|f\rangle$ and the intermediate states $|e\rangle$ become comparable.

IV. PUMP-PROBE WITH TWIN PHOTONS

We now assume that modes $\mathbf{k}_1$ and $\mathbf{k}_2$ are initially prepared in a twin state [41] representing an entangled photon

pair. This can be produced by spontaneous parametric down conversion in a birefringent second-order nonlinear crystal $\chi^{(2)}$. The photon pair is described by a nonseparable wave function even when the photons are physically separated [47],

$$|\psi^{(2)}(0)\rangle = C\sum_{\mathbf{k}_1}\sum_{\mathbf{k}_2} t_I \exp\left(-i\frac{\Delta\omega t_I}{2}\right)\mathrm{sinc}\left(\frac{\Delta\omega t_I}{2}\right) \times\exp\left(-i\frac{(\Delta\mathbf{k})_z L_z}{2}\right)\mathrm{sinc}\left(\frac{(\Delta\mathbf{k})_z L_z}{2}\right)|\mathbf{k}_1,\mathbf{k}_2\rangle. \tag{12}$$

The Fock state $|\mathbf{k}_1,\mathbf{k}_2\rangle$ has one photon in each mode $\mathbf{k}_1$ and $\mathbf{k}_2$; $\Delta\omega=\omega_p-\omega_1-\omega_2$, $\Delta\mathbf{k}=\mathbf{k}_p-\mathbf{k}_1-\mathbf{k}_2$; t_I and L_z are the interaction time and length within the PDC crystal. The normalization factor $C=\chi^{(2)}\mathcal{E}_p/\sqrt{A_{12}}$ is proportional to the nonlinearity of the PDC crystal, the pump electric field amplitude $\mathcal{E}_p$, and the entanglement area A_{12} [24]. The detectors d_1 and d_2 can distinguish between the two modes by their polarization (vertical for $\mathbf{k}_1$ and horizontal for $\mathbf{k}_2$).

For the twin state each of the optical field correlation functions $\langle E^\dagger E^\dagger EE\rangle$ in Eq. (6) is factorized into a product of two field transition amplitudes [47],

$$\begin{aligned}\langle 0,0|E^2(t_4)E^1(t_2)|\psi^{(2)}(0)\rangle &= \theta(t_4-t_2)F(t_4,t_2,T_{12}) + \theta(t_2-t_4)F(t_2,t_4,T_{12})\\ &\times\langle\psi^{(2)}(0)|E^{1\dagger}(t_3)E^{2,\dagger}(t_1)|0,0\rangle\\ &= \theta(t_3-t_1)F^\star(t_3,t_1,T_{12}) + \theta(t_1-t_3)F^\star(t_1,t_3,T_{12}),\end{aligned} \tag{13}$$

where

$$F(t_4,t_2,T_{12}) = \frac{2\pi\chi^{(2)}\mathcal{E}_p}{\Omega}\sqrt{\frac{\omega_1\omega_2}{A_{12}T_{12}}} \times\exp[-i(\omega_1 t_2+\omega_2 t_4)]\mathrm{rect}\left(\frac{t_4-t_2}{T_{12}}\right), \tag{14}$$

$\mathrm{rect}(t)$ is the rectangular function equal to 1 for $0\le t\le 1$ and 0 otherwise, and $T_{12}=(1/v_1-1/v_2)L_z$ is the entanglement time determined by the group velocities $v_1(v_2)$ of the mode $\mathbf{k}_1(\mathbf{k}_2)$ within the PDC crystal.

By substituting Eq. (13) into Eq. (6), we get

$$\begin{aligned}S^{d_2}_{\mathrm{PP}}(\omega_2;\omega_1,T_{12}) = -\frac{4N}{2T}\int_{-T}^{T}dt_4\ \mathrm{Im}\ i^3\int_{-\infty}^{\infty}\int_{-\infty}^{\infty}\int_{-\infty}^{\infty}dt_3dt_2dt_1\\ \times[\theta(t_4-t_2)\theta(t_2-t_3)\theta(t_3-t_1)\langle V(t_1)V(t_3)V^\dagger(t_2)V^\dagger(t_4)\rangle F^\star(t_3,t_1,T_{12})F(t_4,t_2,T_{12})\\ +\theta(t_4-t_2)\theta(t_2-t_1)\theta(t_1-t_3)\langle V(t_3)V(t_1)V^\dagger(t_2)V^\dagger(t_4)\rangle F^\star(t_1,t_3,T_{12})F(t_4,t_2,T_{12})\\ +\theta(t_4-t_2)\theta(t_4-t_3)\theta(t_3-t_1)\langle V(t_1)V(t_3)V^\dagger(t_4)V^\dagger(t_2)\rangle F^\star(t_3,t_1,T_{12})F(t_2,t_4,T_{12})\\ +\theta(t_4-t_2)\theta(t_4-t_1)\theta(t_1-t_3)\langle V(t_3)V(t_1)V^\dagger(t_4)V^\dagger(t_2)\rangle F^\star(t_1,t_3,T_{12})F(t_2,t_4,T_{12})].\end{aligned} \tag{15}$$

We now introduce the Fourier transform of the joined matter and entangled photon Green's functions,

$$I_{eg}(\omega,T_{12}) = -i\int_{-\infty}^{\infty}G_{ee}(\tau)\mathrm{rect}\left(\frac{\tau}{T_{12}}\right)\exp[i(\omega-\omega_g)\tau]d\tau = \frac{e^{i(\omega-\omega_{eg}+i\gamma)T_{12}}-1}{\omega-\omega_{eg}+i\gamma}. \tag{16}$$

By substituting Eqs. (4) and (13) into Eq. (15) and changing the time variables to the loop times, we can express the TPA signal in terms of the entangled photons and matter Green's functions as follows:

$$\begin{aligned}S^{d_2}_{\mathrm{PP}}(\omega_2;\omega_1,T_{12}) = \frac{16\pi^2N|\chi^{(2)}|^2|\mathcal{E}_p|^2\omega_1\omega_2}{A_{12}T_{12}\Omega^2}\mathrm{Im}\sum_{f,e',e}\mu_{e'g}\mu^\star_{eg}\mu_{e'f}\mu^\star_{ef}I^\star_{fg}(\omega_1+\omega_2)[I^\star_{e'g}(\omega_2,T_{12})I^\star_{eg}(\omega_1,T_{12})+I^\star_{e'g}(\omega_2,T_{12})I^\star_{eg}(\omega_2,T_{12})\\ +I_{e'g}(\omega_1,T_{12})I^\star_{eg}(\omega_1,T_{12})+I_{e'g}(\omega_1,T_{12})I^\star_{eg}(\omega_2,T_{12})],\end{aligned} \tag{17}$$

where $I_{fg}(\omega_1+\omega_2)$ is the material doubly excited state Green's function (10). The signal $S^{d_1}_{\mathrm{PP}}(\omega_1;\omega_2,T_{12})$ can be obtained from Eq. (17) by interchanging ω_1 and ω_2.

Introducing the entanglement modified two-photon transition amplitude

$$\mathcal{T}_{gf}(\omega_1,\omega_2,T_{12}) = \mu_{ge}\mu_{ef}I_{eg}(\omega_1,T_{12})+\mu_{ge}\mu_{ef}I_{eg}(\omega_2,T_{12}),$$

$$\mathcal{T}_{fg}(\omega_1,\omega_2,T_{12}) = \mu^\star_{ge}\mu^\star_{ef}I_{eg}(\omega_1,T_{12})+\mu^\star_{ge}\mu^\star_{ef}I_{eg}(\omega_2,T_{12}), \tag{18}$$

we obtain the symmetric TPA signal induced by the twin photons,

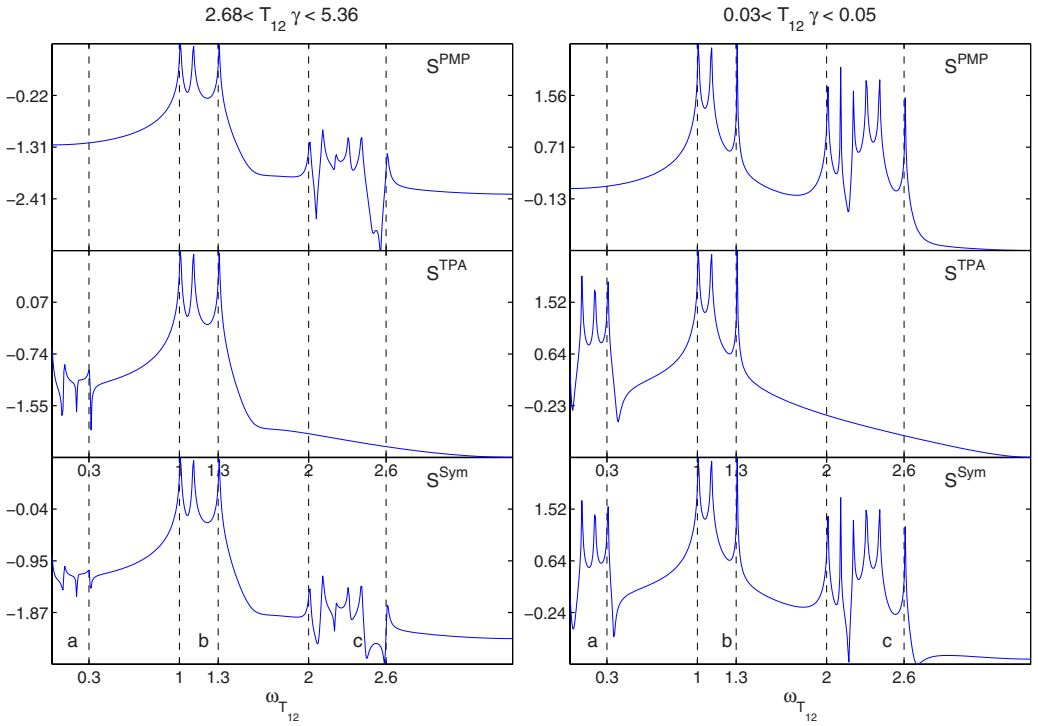

FIG. 3. (Color online) The pump-probe spectra $\log_{10}|S^{\nu}_{\mathrm{TPA}}(\omega_p/2,\omega_T)|$ [Eq. (25)]. The signals recorded by the two detectors are identical $S^{d_1}=S^{d_2}=S^{\mathrm{Sym}}$. Left (right) column correspond to large (small) dephasing rate, as shown.

$$S^{\mathrm{Sym}}_{\mathrm{PP}}(\omega_1,\omega_2,T_{12}) = \frac{8\pi^2 N|\chi^{(2)}|^2|\mathcal{E}_p|^2\omega_1\omega_2}{A_{12}T_{12}\Omega^2} \times \mathrm{Im}\, I^{\star}_{fg}(\omega_1+\omega_2)[\mathcal{T}^{\star}_{gf}(\omega_1,\omega_2,T_{12}) \times \mathcal{T}^{\star}_{fg}(\omega_1,\omega_2,T_{12}) + |\mathcal{T}_{fg}(\omega_1,\omega_2,T_{12})|^2]. \tag{19}$$

As in Eq. (11), the two terms correspond to PMP and TPA pathways. It is interesting to note that the symmetric PP signal generated by twin photons (19) may not be described by the absolute square of the transition amplitude.

We have carried out simulations for the following model material system. The single excited state frequencies $\omega_{eg}=\{1.5,1.6,1.8\}$ are off resonant $(\omega_{eg}-\omega_p/2)T_{12}\gg\gamma T_{12}$. The doubly excited state at $\omega_{fg}=1$ is resonant with the pump photon $\omega_{gf}=\omega_p$ used to generate the degenerate twins $\omega_1=\omega_2=\omega_p/2$. All dipole moments are real and identical.

We have varied the entanglement time T_{12} from $T_{\min}=2^{12}\Delta T_{12}$ to $T_{\max}=2T_{\min}$ with the time stem $\Delta T_{12}=2\pi/[\max(\omega_{eg}+\omega_{e'g}-\omega_p)]=0.025$. That is if the unit of energy is $\hbar\omega_p=1$ eV then $\Delta\tau=1.3$ fs. This can be done by tilting the PDC crystal [36] which increases its size L_z.

In Fig. 3 we display the entanglement time spectra defined as follows:

$$S^{\nu}_{\mathrm{PP}}(\omega_p/2,\omega_T) = \mathcal{N}\int_{T_{\min}}^{T_{\max}} dT_{12}\exp(i\omega_{T_{12}}T_{12})S^{\nu}_{\mathrm{PP}}(\omega_p/2,T_{12}), \tag{20}$$

where superscript ν can be $\{d1,d2,\mathrm{Sym},\mathrm{TPA},\mathrm{PMP}\}$ and $\mathcal{N}=1/S^{\mathrm{Sym}}_{\mathrm{TPA}}(\omega_p/2,T_{12})$ is a normalization factor. The spectra show several groups of resonances. Group a correspond to the intraband resonances of the intermediate-state manifold $0\le\omega_{T_{12}}=\omega_{eg}-\omega_{e'g}\le 0.3$, group b corresponds to the $1\le\omega_{T_{12}}=\omega_{eg}-\omega_p/2\le 1.3$ resonances, and group c describes $2\le\omega_{T_{12}}=\omega_{eg}+\omega_{e'g}-\omega_p\le 2.6$ resonances. Note that the resonances of group b can be detected by a conventional pump probe with short well-separated classical pulses.

All pathways (Fig. 2) which contribute to the signals interfere constructively. The left column in Fig. 3 uses a larger dephasing rate $2.68<T_{12}\gamma<5.36$ than the right column $0.03<\gamma T_{12}<0.05$. The larger dephasing rate in the left column quenches the resonances in regions a and c. PMP pathways contribute to spectral regions b and c, while TPA pathways show resonances in regions i and ii. We note that for this technique $S^{d_1}=S^{d_2}=S^{\mathrm{Sym}}$ and the asymmetric signal S^{Asym} vanishes. In both columns the S^{TPA} signal has no resonances in region c whereas the S^{PMP} signal does not show resonances in region a.

V. PUMP-PROBE WITH MUTUALLY DELAYED TWIN PHOTONS

We next turn to a more general twin photon PP setup as proposed by Saleh *et al.* [32]. The twins remain degenerate $\omega_1=\omega_2=\omega_p/2$ but we introduce a relative time delay $0<\tau<T_{12}$ between them by shifting the phase of the $\mathbf{k}_1$ mode [12,40],

$$E_1(t) = \left(\frac{\pi\omega_p}{\Omega}\right)^{1/2} a_1 \exp[-i\omega_p(t-\tau/2)/2],$$

$$E_2(t) = \left(\frac{\pi\omega_p}{\Omega}\right)^{1/2} a_2 \exp[-i\omega_p(t+\tau/2)/2]. \quad (21)$$

Using Eq. (21) we obtain the optical field transition amplitudes for diagrams i–iv,

$$\langle 0,0|E_2(t_4)E_1(t_2)|\psi^{(2)}(0)\rangle = \theta(t_4-t_2)F(t_4,t_2,T_{12}) + \theta(t_2-t_4)F(t_2,t_4,T_{12}),$$

$$\langle \psi^{(2)}(0)|E_1^\dagger(t_3)E_2^\dagger(t_1)|0,0\rangle = \theta(t_3-t_1)F^\star(t_3,t_1,T_{12}) + \theta(t_1-t_3)F^\star(t_1,t_3,T_{12}), \quad (22)$$

where

$$F(t_4,t_2,T_{12}) = \frac{\pi\chi^{(2)}\mathcal{E}_p\omega_p}{\Omega\sqrt{A_{12}T_{12}}}\exp[-i\omega_p/2(t_4+t_2)]\mathrm{rect}\left(\frac{t_4-t_2}{T_{12}-\tau}\right).$$

For diagrams v–viii one has to interchange $t_4 \leftrightarrow t_2, t_3 \leftrightarrow t_1$ in the above expression.

The signal in Eq. (15) now becomes

$$S_{\mathrm{PP}}^{d_2}(\omega_p/2,T_{12},\tau) = \frac{16\pi^2 N|\chi^{(2)}|^2|\mathcal{E}_p|^2\omega_p^2}{A_{12}T_{12}\Omega^2}\mathrm{Im}\sum_{f,e',e}\mu_{e'g}\mu_{eg}^\star\mu_{e'f}\mu_{ef}^\star I_{fg}^\star(\omega_p)[I_{e'g}^\star(\omega_p/2,T_{12}-\tau)I_{eg}^\star(\omega_p/2,T_{12}-\tau) + I_{e'g}^\star(\omega_p/2,T_{12}-\tau)I_{eg}^\star(\omega_p/2,T_{12}+\tau) + I_{e'g}(\omega_p/2,T_{12}-\tau)I_{eg}^\star(\omega_p/2,T_{12}-\tau) + I_{e'g}(\omega_p/2,T_{12}-\tau)I_{eg}^\star(\omega_p/2,T_{12}+\tau)]. \quad (23)$$

The signal from the other detector is $S_{\mathrm{PP}}^{d_1}(\omega_p/2,T_{12},\tau) = S_{\mathrm{PP}}^{d_2}(\omega_p/2,T_{12},-\tau)$. Here $I_{eg}(\omega_p/2,T_{12}\mp\tau)$ describes the Fourier transform of the system (twin+matter) Green's function which depends on the delay τ between the entangled photons. This delay breaks the symmetry of the process making it dependent on the order in which the twins are absorbed or emitted even in the degenerate case [see Fig. 1(c)]. If mode $\mathbf{k}_1$ precedes $\mathbf{k}_2$, the system's evolution is described by the following Green's function: $I_{eg}(\omega,T_{12}-\tau)$. When $\mathbf{k}_2$ comes first we have $I_{eg}(\omega,T_{12}+\tau)$. The broken symmetry implies that $S_{\mathrm{PP}}^{d_2}(\omega_p/2,T_{12},\tau) \neq S_{\mathrm{PP}}^{d_1}(\omega_p/2,T_{12},\tau)$.

Using the field transition amplitudes (22) the two-photon transition amplitude assumes the form

$$\mathcal{T}_{gf}(\omega_p/2,T_{12},\tau) = \sum_e \mu_{ge}\mu_{ef}I_{eg}(\omega_p/2,T_{12}-\tau) + \mu_{ge}\mu_{ef}I_{eg}(\omega_p/2,T_{12}+\tau),$$

$$\mathcal{T}_{fg}(\omega_p/2,T_{12},\tau) = \sum_e \mu_{ge}^\star\mu_{ef}^\star I_{eg}(\omega_p/2,T_{12}-\tau) + \mu_{ge}^\star\mu_{ef}^\star I_{eg}(\omega_p/2,T_{12}+\tau). \quad (24)$$

The symmetrized signal (3) can be written in terms of the matter field transition amplitudes (24) as

$$S_{\mathrm{PP}}^{\mathrm{Sym}}(\omega_p/2,T_{12},\tau) = \tfrac{1}{2}[S_{\mathrm{PP}}^{\mathrm{PMP}}(\omega_p/2,T_{12},\tau) + S_{\mathrm{TPA}}^{\mathrm{Sym}}(\omega_p/2,T_{12},\tau)], \quad (25)$$

where

$$S_{\mathrm{PP}}^{\mathrm{PMP}}(\omega_p/2,T_{12},\tau) = \frac{16\pi^2 N|\chi^{(2)}|^2|\mathcal{E}_p|^2\omega_p^2}{A_{12}T_{12}\Omega^2} \times \mathrm{Im}\sum_f I_{fg}^\star(\omega_p)\mathcal{T}_{fg}^\star(\omega_p/2,T_{12},\tau) \times \mathcal{T}_{gf}^\star(\omega_p/2,T_{12},\tau), \quad (26)$$

$$S_{\mathrm{PP}}^{\mathrm{TPA}}(\omega_p/2,T_{12},\tau) = \frac{16\pi^2 N|\chi^{(2)}|^2|\mathcal{E}_p|^2\omega_p^2}{A_{12}T_{12}\Omega^2} \times \sum_f |\mathcal{T}_{fg}(\omega_p/2,T_{12},\tau)|^2\delta(\omega_p-\omega_{fg}). \quad (27)$$

Equation (27) is identical to the result of Ref. [32]. For the degenerate case $\omega_1=\omega_2$, the symmetry of the above signal implies the following symmetry with respect to the time delay $S_{\mathrm{PP}}^{\mathrm{Sym}}(\omega_p/2,T_{12},\tau)=S_{\mathrm{PP}}^{\mathrm{Sym}}(\omega_p/2,T_{12},-\tau)$.

We next turn to the antisymmetric signal [the difference between the detector d_1 and d_2 in Fig. 1(a)],

$$S_{\mathrm{PP}}^{\mathrm{Asym}}(\omega_p/2,T_{12},\tau) = \frac{8\pi^2 N|\chi^{(2)}|^2|\mathcal{E}_p|^2\omega_p^2}{A_{12}T_{12}\Omega^2}\mathrm{Im}\sum_f I_{fg}^\star(\omega_p) \times [\mathcal{T}_{gf}^\star(\omega_p/2,T_{12},\tau)\mathcal{T}_{gf}'^\star(\omega_p/2,T_{12},\tau) + \mathcal{T}_{gf}'(\omega_p/2,T_{12},\tau)\mathcal{T}_{fg}^\star(\omega_p/2,T_{12},\tau)]. \quad (28)$$

Here we have introduced the antisymmetric two-photon transition amplitude

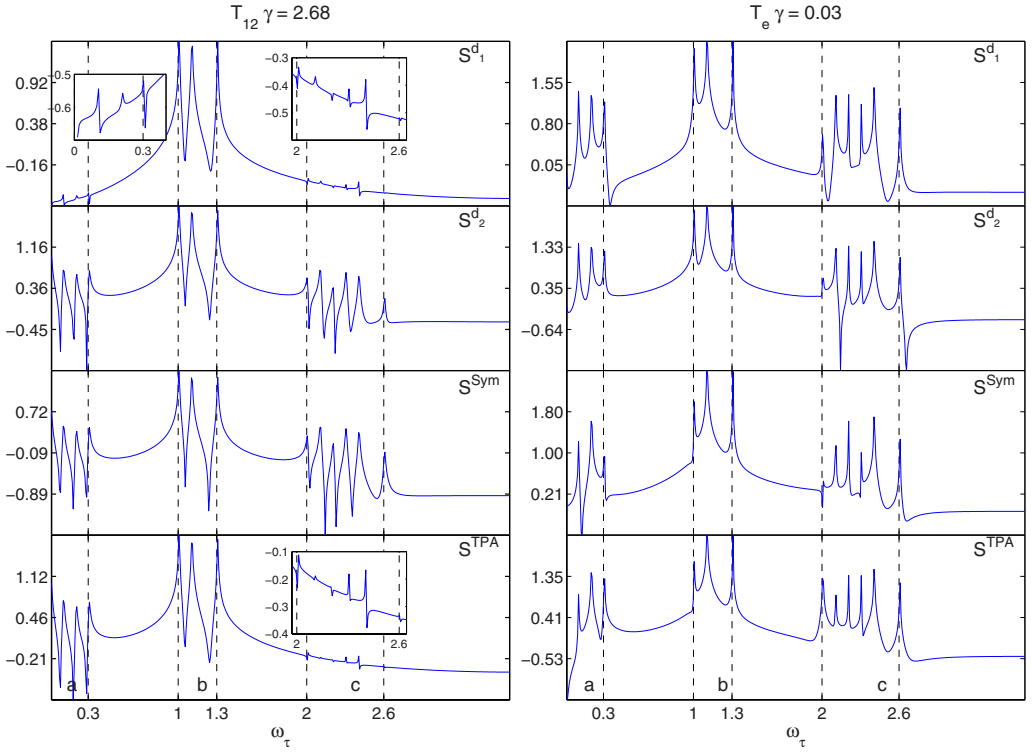

FIG. 4. (Color online) The pump-probe spectra $\log_{10}|S^{\nu}_{\mathrm{TPA}}(\omega_p/2,T_{12},\omega_\tau)|$ vs ω_τ and a fixed entanglement time T_{12}. The two columns differ by the dephasing rate, as indicated.

$$\mathcal{T}'_{gf}(\omega_p/2,T_{12},\tau)=\sum_e \mu_{ge}\mu_{ef}I_{eg}(\omega_p/2,T_{12}-\tau) - \mu_{ge}\mu_{ef}I_{eg}(\omega_p/2,T_{12}+\tau). \quad (29)$$

This signal vanishes in frequency-domain experiments with classical fields where the order in which the modes interact is not important,

$$\mathcal{T}'_{gf}(\omega_1,\omega_2)=\mu_{ge}\mu_{ef}I_{eg}(\omega_1,\omega_2)-\mu_{ge}\mu_{ef}I_{eg}(\omega_1,\omega_2)=0.$$

The asymmetric signal also vanishes at zero twin photon delay since $\mathcal{T}'_{gf}(\omega_p/2,T_{12},0)=0$. Absorption of $\mathbf{k}_1$ is always accompanied by absorption of $\mathbf{k}_2$ and the same holds for emission. For the twin photons with delay τ the Green's functions do depend on the order of interaction and the asymmetric signal does not vanish. This signal is thus induced by the delay between twin photons.

In Fig. 4 we compare the individual detector readings (23), the symmetrized signal (25), and the TPA contribution (27) to the PP signal. First, we hold the entanglement time T_{12} fixed and plot the Fourier transforms with respect to the time delay τ:

$$S^{\nu}_{\mathrm{PP}}(\omega_p/2,T_{12},\omega_\tau)=\mathcal{N}\int_0^{T_{12}} d\tau\exp(i\omega_\tau\tau)S^{\nu}_{\mathrm{PP}}(\omega_p/2,T_{12},\tau). \quad (30)$$

The entanglement time increases from zero with a step $\Delta\tau\Delta T_{12}$ up to the value of the entanglement time $T_{12}=T_{\min}$. As in Fig. 3 the resonances of the entanglement time PP spectra may be classified by the same three spectral groups a,b,c. Recall that the spectra with respect to the entanglement time associate the region a with PMP and region c with TPA. However their meanings for the spectra given by Eq. (30) is quite different. For PMP pathways region a resonances are produced by the pathways i, v, iii, and vii where emitted and absorbed photons follow the same chronological order; the region b resonances are given by the pathways ii, vi, iv, and viii where the chronological photon order for the emission is opposite to those of the absorption. For TPA the meaning of the regions of a and c is exactly opposite to those of PMP. This peculiar feature is a result of broken symmetry of the field transition amplitude. For small dephasing rate $\gamma T_{12}=0.03$ (right column) PMP and TPA contribute to the same regions in all spectra and spectrally nonseparable by the pump-probe technique. At large dephasing rate $\gamma T_{12}=2.68$ (left column) pathways v–viii do not contribute to regions a and c. PMP pathways i and ii contribute to the spectral regions b and c while TPA pathways iii and iv contribute to regions a and b. We note that the spectra obtained from the two detectors are different $S^{d_1}\neq S^{d_2}$. Only the S^{d_2} signal shows resonances in the nonclassical regions a and c. However, both S^{Sym} and S^{Asym} signals contain all resonances. The TPA signal misses the region c resonances and PMP misses resonances in region a; thus, one can separate PMP from TPA if focuses on the regions a and c only.

In Fig. 5 we display correlation 2D spectra between the entanglement and the delay times,

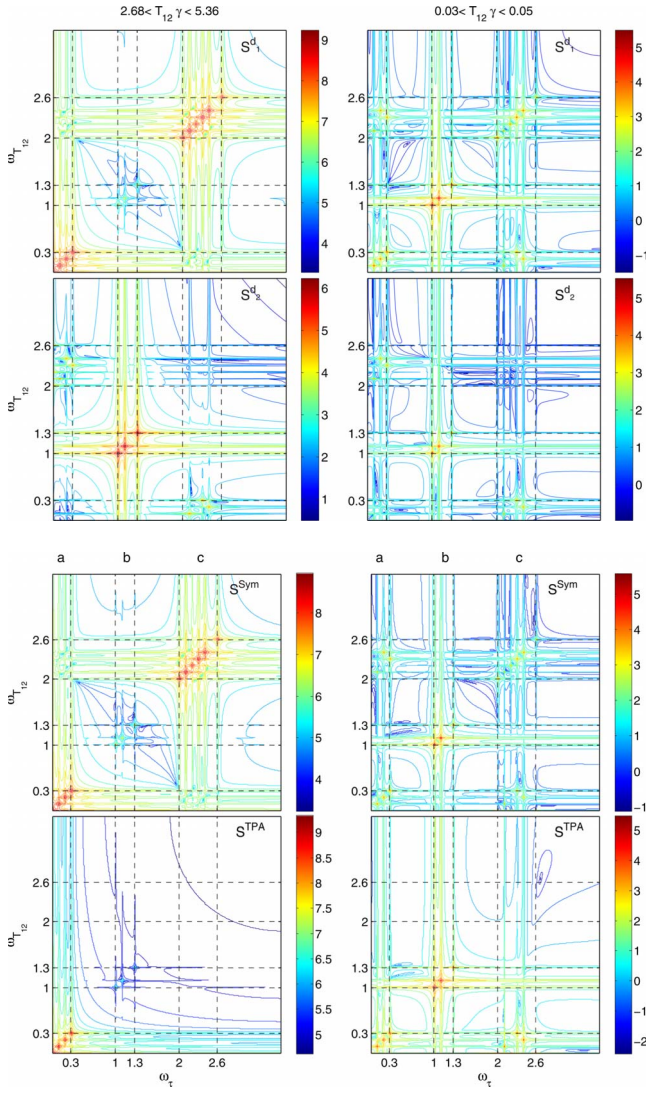

FIG. 5. (Color online) 2D correlation pump-probe spectra $\log_{10}|S^{\nu}_{\mathrm{TPA}}(\omega_p/2,\omega_{T_{12}},\omega_\tau)|$ with entangled twin photons. The left and right columns represent different dephasing rates.

$$S^{\nu}_{\mathrm{TPA}}(\omega_p/2,\omega_{T_{12}},\omega_\tau)=\mathcal{N}\int_{T_{\min}}^{T_{\max}} dT_{12}\,\exp(i\omega_{T_{12}}T_{12})$$

$$\times\int_0^{T12} d\tau\,\exp(i\omega_\tau\tau)S^{\nu}_{\mathrm{TPA}}(\omega_p/2,T_{12},\tau). \tag{31}$$

The resonances are classified into five regions in the $(\omega_{T_{12}},\omega_\tau)$ plane. The PMP pathways contribute to regions (b,b), (c,a), and (c,c); the TPA pathways create resonances at (a,a), (b,b), and (a,c). Therefore regions a,c and pathways c,a directly show the correlation between the PMP and TPA. We find that for both values of the dephasing rate the TPA and PMP signals miss the (c,c) and (a,a) resonances correspondingly. The correlation spectra from the two detectors are different. Unlike the delay spectra, detector d_1 reveals all spectral regions, while resonances (a,a) and (c,c) from detector d_2 are suppressed. Finally the off-diagonal, as well as (b,b), resonances are sensitive to the dephasing rate and vanish for large dephasing. The diagonal (a,a) and (c,c) resonances overlap as the dephasing rate is increased. In summary, the conventional frequency-domain PP signal when ω_1 and ω_2 are off resonant can be described as a two-photon counting process. The twin photons characterized by their frequencies, polarizations, and the entanglement time T_{12} generate the symmetric PP signal [Eq. (19)] obtained from CTPL formalism. The signal consists of TPA $\sim|\mathcal{T}_{fg}(T_{12})|^2$ as well as PMP $\sim\mathcal{T}^{\star}_{gf}(T_{12})\mathcal{T}^{\star}_{fg}(T_{12})$ terms. The two terms may be observed separately by measuring two-photon-induced fluorescence from the doubly and singly excited states, respectively. Alternatively, they can be spectrally separated by focusing on certain regions in $S^{\mathrm{Sym}}_{\mathrm{PP}}(\omega_p/2,\omega_{T_{12}})$. When the time delay τ is introduced the two detectors yield two different signals $S^{d_{1,2}}_{\mathrm{PP}}(\omega_p/2,\omega_\tau)$ giving rise to the asymmetric signal $S^{\mathrm{Asym}}_{\mathrm{PP}}(\omega_p/2,\omega_\tau)$ or spectra. For $S^{\mathrm{Sym}}_{\mathrm{PP}}(\omega_p/2,\omega_\tau)$ the separation between PMP and TPA is possible only at large dephasing. The correlation between PMP and TPA pathways can be seen in the off-diagonal regions on the 2D correlation spectra $S^{\nu}_{\mathrm{PP}}(\omega_p/2,\omega_{T_{12}},\omega_\tau)$. Spectral separation and correlation between PMP and TPA is important if the direct observation of the fluorescence from $|e\rangle$ or $|f\rangle$ is not possible due to selection rules or fast nonradiative relaxation of the $|f\rangle$ state.

VI. PUMP-PROBE WITH RECTANGULARLY SHAPED CLASSICAL OPTICAL FIELDS

We now demonstrate how similar spectra can be obtained with shaped classical pulses. The key ingredients of the TPA signals are the optical field transition amplitudes, which can be shaped and manipulated. Let us assume that modes $\mathbf{k}_1$ and $\mathbf{k}_2$ are created from a rectangular (width T_{12}) pump beam with frequency ω_p by means of 50:50 beam splitter. Both modes are classical and initially in a coherent state $|\beta\rangle$. The beam-splitter-induced $\pi/2$ phase shift between the reflected $\mathbf{k}_1$ and transmitted $\mathbf{k}_2$ modes can be compensated by difference in their optical path from the splitter to the sample. We further introduce relative time delay τ in $\mathbf{k}_1$ beam path. The optical field operators are

$$E_1(t)=\left(\frac{2\pi\omega_p}{\Omega}\right)^{1/2} a_1\exp[-i\omega_p(t-\tau/2)/2]$$
$$\times\mathrm{rect}\left(\frac{t-\tau/2-T_{12}/2}{T_{12}}\right),$$

$$E_2(t)=\left(\frac{2\pi\omega_p}{\Omega}\right)^{1/2} a_2\exp[-i\omega_p(t+\tau/2)/2]$$
$$\times\mathrm{rect}\left(\frac{t+\tau/2-T_{12}/2}{T_{12}}\right). \tag{32}$$

Making use of the following identity:

$$\mathrm{rect}\left(\frac{t_4-\tau/2-T_{12}/2}{T_{12}}\right)\mathrm{rect}\left(\frac{t_2+\tau/2-T_{12}/2}{T_{12}}\right)$$
$$=\mathrm{rect}\left(\frac{|t_4-t_2+\tau|}{T_{12}}\right),$$

we obtain the following field transition amplitudes for diagrams i–iv:

$$\begin{aligned}
&\langle\beta_1,\beta_2|E^2(t_4)E^1(t_2)|\beta_1,\beta_2\rangle\\
&\quad=\theta(t_4-t_2)E(t_4,t_2,T_{12})+\theta(t_2-t_4)E(t_2,t_4,T_{12})\\
&\quad=\frac{2\pi\omega_p}{\Omega}\exp[-i\omega_p/2(t_4+t_2)]\\
&\qquad\times\left[\theta(t_4-t_2)\mathrm{rect}\left(\frac{t_4-t_2}{T_{12}-\tau}\right)+\theta(t_2-t_4)\mathrm{rect}\left(\frac{t_2-t_4}{T_{12}+\tau}\right)\right],\\
&\langle\beta_1,\beta_2|E^{1\dagger}(t_3)E^{2,\dagger}(t_1)|\beta_1,\beta_2\rangle\\
&\quad=\theta(t_3-t_1)E^\star(t_3,t_1,T_{12})+\theta(t_1-t_3)E^\star(t_1,t_3,T_{12})\\
&\quad=\frac{2\pi\omega_p}{\Omega}\exp[i\omega_p/2(t_3+t_1)]\\
&\qquad\times\left[\theta(t_3-t_1)\mathrm{rect}\left(\frac{t_3-t_1}{T_{12}-\tau}\right)+\theta(t_1-t_3)\mathrm{rect}\left(\frac{t_1-t_3}{T_{12}+\tau}\right)\right].
\end{aligned}\tag{33}$$

Substituting Eq. (33) into Eq. (15) gives

$$S^{\mathrm{Sym}}_{\mathrm{TPA}}(\omega_p/2,T_{12},\tau)=\frac{16\pi^2N\omega_p^2}{\Omega^3 2}\mathrm{Im}\,I^\star_{fg}(\omega_p)[\mathcal{T}^{\star,2}_{fg}(\omega_p/2,T_{12},\tau)+|\mathcal{T}_{fg}(\omega_p,T_{12},\tau)|^2]\tag{34}$$

Equation (34) derived for shaped classical modes coincides with the entanglement-induced TPA signal [Eq. (25)] up to an overall scaling factor. Equation (25) scales linearly with the pump photon intensity, while the classical signal scales quadratically. The scaling factor is independent on the τ parameter. Therefore their Fourier spectra with respect to τ are identical.

Pump-probe spectroscopy performed with shaped classical pulses where the pump is split into two copropagating pulses separated by a delay τ gives information equivalent to four-wave mixing carried out with four pulses. 2D spectra can be obtained by, e.g., varying τ and the T_{12}. The twin delay τ plays a similar role but enters in a different way than with classical fields. The precise connection between the two approaches to multidimensional spectroscopy based controlling either the delays between classical pulses or the parameters of entangled photon wave function that determine their relative timing statistics will be an interesting topic for future investigations.

VII. CONCLUSIONS

In this paper we demonstrated how quantum degrees of freedom of the radiation field may be used as multidimensional spectroscopic probes of matter. Mutually delayed twin photons tuned to two-photon resonances $\omega_1+\omega_2=\omega_{fg}$ can provide direct information on off-resonant transitions. The twin photon state is a wave packet of two groups of modes that can be distinguished and detected separately by two detectors d_1 and d_2 by exploiting their different polarizations or propagation directions. The two detectors measure the intensity change in one of the beams with and without the sample. An intuitive microscopic formalism based on close time path loop (CTPL) diagrams is developed and employed to calculate the pump-probe signals generated with the entangled photons $S^{d_1}_{\mathrm{PP}}$ and $S^{d_2}_{\mathrm{PP}}$. Symmetric (asymmetric) signals are further defined as the sum (difference) of the detector readings ($S^{d_1}_{\mathrm{PP}}\pm S^{d_2}_{\mathrm{PP}}$). For general quantum optical fields the signal is recast in terms of quantum pathways of matter, each scaled with a corresponding four-point field correlation functions. Such signals may not be expressed in terms of ordinary *causal* response functions and susceptibilities as is the case for classical fields since they depend on correlated spontaneous fluctuations of field and matter. For classical fields the signal is given by a product of a susceptibility and field amplitude. In the entangled case the signal is given by a sum of such products. The symmetrized pump-probe signal can be divided into components which represent two groups of pathways $S^{\mathrm{PMP}}_{\mathrm{PP}}+S^{\mathrm{TPA}}_{\mathrm{PP}}$. TPA may be measured by fluorescence from the doubly excited states $|f\rangle$ and may be calculated as a modulus square of a two-photon counting amplitude. PMP on the other hand represents a process where one of the pump photon creates an intermediate coherence between the ground and double excited states and "catalyzes" the probe absorption, without changing its state at the end of the process. This component can be measured by fluorescence from the singly excited $|e\rangle$ state and is given by the imaginary part of a product of two-photon complex transition amplitudes (not modulus square). For classical off-resonant fields $S^{\mathrm{PMP}}_{\mathrm{PP}}=S^{\mathrm{TPA}}_{\mathrm{PP}}$, and the antisymmetric signal $S^{\mathrm{Asym}}_{\mathrm{PP}}$ vanishes. However it becomes finite with twin photons. The distinction between the pump-probe and TPA signals has not been clearly made in the literature, where the two terms are used interchangeably. 2D signals obtained by varying the delay time τ and the entanglement time T_{12} reveal the off-resonant singly excited state frequencies and allow us to distinguish between various groups of resonances. Focusing on different regions of the spectra one can separate PMP and TPA contributions or measure the correlation between the two. This spectral resolution is especially important if direct measurement of the fluorescence from the $|f\rangle$ is impossible. We further showed that one can mimic the entangled-photon pump-probe signals by using two mutually delayed rectangularly shaped *classical* optical fields. The present formalism allows us to describe pulse shaping and photon entanglement within the same framework. This may allow the design of other types of time-domain spectroscopies which make use of the broad band width of entangled photons to probe relaxation processes in the resonantly excited states.

ACKNOWLEDGMENTS

This work was supported by the National Science Foundation Grant No. CHE-0745892 and the National Institutes of Health Grant No. GM59230.

[1] R. Ernst, G. Bodenhausen, and A. Wokaun, *Principles of Nuclear Magnetic Resonance in One and Two Dimensions* (Clanderon Press, Oxford, 1998).
[2] S. Mukamel, Annu. Rev. Phys. Chem. **51**, 691 (2000).
[3] M. Asplund, M. Zanni, and R. Hochstrasser, Proc. Natl. Acad. Sci. U.S.A. **97**, 8219 (2000).
[4] S. Mukamel, D. Abramavicius, Lijun Yang, Wei Zhuang, I. V. Schweigert, and D. V. Voronine, Acc. Chem. Res. (to be published).
[5] G. S. Engel, T. R. Calhoun, E. L. Read, T. K. Ahn, T. Mancal, Y. C. Cheng, R. E. Blankenship, and G. R. Fleming, Nature (London) **446**, 782 (2007).
[6] D. Oron, N. Dudovich, and Y. Silberberg, Phys. Rev. Lett. **90**, 213902 (2003).
[7] H. Li, D. Ahmasi, H. B. Xu, P. J. Wrzesinski, V. V. Lozovoy, and M. Dantus, Opt. Photonics News **19**, 46 (2008).
[8] S. Postma, A. C. Van Rhijn, J. P. Korterik, P. Gross, J. L. Herek, and H. L. Offerhaus, Opt. Express **16**, 7985 (2008).
[9] L. P. DeFlores, R. A. Nicodemus, and A. Tokmakoff, Opt. Lett. **32**, 2966 (2007).
[10] E. M. Grumstrup, S. H. Shim, M. A. Montgomery, N. H. Damrauer, and M. T. Zanni, Opt. Express **15**, 16681 (2007).
[11] J. A. Myers, K. L. Lewis, P. F. Tekavec, and J. P. Ogilvie, Opt. Express **16**, 17420 (2008).
[12] K. Edamatsu, Jpn. J. Appl. Phys. **46**, 7175 (2007).
[13] C. K. Hong and L. Mandel, Phys. Rev. A **31**, 2409 (1985).
[14] A. Furusawa, J. L. Sørensen, S. L. Braunstein, C. A. Fuchs, H. J. Kimble, and E. S. Polzik, Science **282**, 706 (1998).
[15] N. Gisin, G. Ribordy, W. Tittel, and H. Zbinden, Rev. Mod. Phys. **74**, 145 (2002).
[16] M. Scully and M. Zubairy, *Quantum Optics* (Cambridge University Press, Cambridge, UK, 1997).
[17] A. Aspect, P. Grangier, and G. Roger, Phys. Rev. Lett. **49**, 91 (1982).
[18] S. Haroche and J. Raimond, *Exploring the Quantum: Atoms, Cavities, and Photons* (Oxford University Press, New York, 2006).
[19] P. G. Kwiat, K. Mattle, H. Weinfurter, A. Zeilinger, A. V. Sergienko, and Y. Shih, Phys. Rev. Lett. **75**, 4337 (1995).
[20] E. S. Fry and R. C. Thompson, Phys. Rev. Lett. **37**, 465 (1976).
[21] A. Aspect, P. Grangier, and G. Roger, Phys. Rev. Lett. **47**, 460 (1981).
[22] S. Yu and J. H. Eberly, Science **323**, 598 (2009).
[23] L. Mandel and E. Wolf, *Optical Coherence and Quantum Optics* (Cambridge University Press, Cambridge, England, 1995).
[24] C. Gerry and P. Knight, *Introductory Quantum Optics* (Cambridge University Press, Cambridge, England, 2005).
[25] M. Fiorentino, P. L. Voss, J. E. Sharping, and P. Kumar, IEEE Photonics Technol. Lett. **14**, 983 (2002).
[26] K. Inoue and K. Shimizu, Jpn. J. Appl. Phys. **43**, 8048 (2004).
[27] K. Edamatsu, G. Oohata, R. Shimizu, and T. Itoh, Nature (London) **431**, 167 (2004).
[28] R. M. Stevenson, A. J. Hudson, R. J. Young, P. Atkinson, K. Cooper, D. A. Ritchie, and A. J. Shields, Opt. Express **15**, 6507 (2007).
[29] J. T. Barreiro, N. K. Langford, N. A. Peters, and P. G. Kwiat, Phys. Rev. Lett. **95**, 260501 (2005).
[30] M. Barbieri, C. Cinelli, P. Mataloni, and F. De Martini, Phys. Rev. A **72**, 052110 (2005).
[31] B. Dayan, A. Peer, A. A. Friesem, and Y. Silberberg, Phys. Rev. Lett. **93**, 023005 (2004).
[32] B. E. A. Saleh, B. M. Jost, H. B. Fei, and M. C. Teich, Phys. Rev. Lett. **80**, 3483 (1998).
[33] B. Dayan, A. Pe'er, A. A. Friesem, and Y. Silberberg, Phys. Rev. Lett. **94**, 043602 (2005).
[34] A. Pe'er, Y. Bromberg, B. Dayan, Y. Silberberg, and A. A. Friesem, Opt. Express **15**, 8760 (2007).
[35] A. Pe'er, B. Dayan, A. A. Friesem, and Y. Silberberg, Phys. Rev. Lett. **94**, 073601 (2005).
[36] M. R. Harpham, O. Suzer, C.-Q. Ma, P. Bauerle, and T. Goodson, J. Am. Chem. Soc. **131**, 973 (2009).
[37] D. Lee and T. Goodson III, Proc. SPIE **6653**, 66530V (2007).
[38] D. Lee and T. Goodson, J. Phys. Chem. B **110**, 25582 (2006).
[39] Ö. Süzer and T. Goodson, Opt. Express **16**, 20166 (2008).
[40] M. Teich and B. Saleh, U.S. Patent 5,796,477 (18 August 1998).
[41] H. B. Fei, B. M. Jost, S. Popescu, B. E. A. Saleh, and M. C. Teich, Phys. Rev. Lett. **78**, 1679 (1997).
[42] J. Javanainen and P. L. Gould, Phys. Rev. A **41**, 5088 (1990).
[43] A. F. Abouraddy, B. E. A. Saleh, A. V. Sergienko, and M. C. Teich, Phys. Rev. Lett. **87**, 123602 (2001).
[44] M. B. Nasr, B. E. A. Saleh, A. V. Sergienko, and M. C. Teich, Phys. Rev. Lett. **91**, 083601 (2003).
[45] O. Roslyak, C. Marx, and S. Mukamel, Phys. Rev. A **79**, 033832 (2009).
[46] O. Roslyak and S. Mukamel, Opt. Express **17**, 1093 (2009).
[47] J. Peřina, Jr., B. E. A. Saleh, and M. C. Teich, Phys. Rev. A **57**, 3972 (1998).
[48] C. A. Marx, U. Harbola, and S. Mukamel, Phys. Rev. A **77**, 022110 (2008).
[49] O. Roslyak, C. Marx, and S. Mukamel, Mol. Phys. (to be published).
[50] R. Glauber, *Quantum Theory of Optical Coherence: Selected Papers and Lectures* (Wiley-VCH, New York, 2007).
[51] U. Harbola and S. Mukamel, Phys. Rep. **465**, 191 (2008).
[52] S. Mukamel, *Principles of Nonlinear Optical Spectroscopy* (Oxford University Press, New York, 1995).
[53] N. Ph. Georgiades, E. S. Polzik, and H. J. Kimble, Phys. Rev. A **59**, 676 (1999).
[54] D. T. Smithey, M. Beck, M. Belsley, and H. G. Raymer, Phys. Rev. Lett. **69**, 2650 (1992).